

Removal of Methylene Blue Dye from Aqueous Solutions by Bentonite and Cement Kiln Dust: Comparative Study of Adsorption Equilibrium, Kinetic, and Thermodynamic

Ahmed A. El-Refaey¹

ABSTRACT

This study compared the methylene blue (MB) removal from aqueous solution by natural bentonite (Bent) and cement kiln dust (CKD). Bentonite and CKD were characterized by X-ray diffraction (XRD), X-ray fluorescence (XRF), Brunauer Emmett Teller (BET) specific surface area, Fourier transform infrared (FTIR), and scanning electron microscopy (SEM). The comparison between bentonite and CKD in the removal of MB dye was investigated in different conditions including initial MB concentration, adsorbent doses, pH, salt concentration, and temperature by batch experiments. Adsorption kinetics results were fitted with fractional power, Elovich, pseudo-first-order, pseudo-second-order, and intra-particle diffusion equations. The pseudo-second-order model was well fitted for experimental results at the different tested initial concentrations (50-300 mgMB/L). Equilibrium adsorption data were evaluated by Freundlich and Langmuir and Temkin models. The experimental results fitted very well by the Langmuir isotherm model. Bentonite exhibited the largest adsorption capacity (3257.33 mg/g) than CKD (2150.54 mg/g). Increasing the temperature from 298K to 323 °K convinced an increase of the adsorption of MB dye by both sorbents and the process was found to be endothermic and spontaneous. The obtained results indicated that both adsorbents are efficient and low-cost adsorbents for effective removal of MB dye with privilege in the efficiency for bentonite and with no cost for CKD.

Keywords: Bentonite; Cement Kiln Dust; methylene blue; kinetic and adsorption isotherm; Thermodynamic.

INTRODUCTION

Dyes are one of the serious aquatic environmental threaten. More than 100,000 dyes used in several industries such as textile, leathers, paint, paper, plastics, food, cosmetics, pharmaceuticals, etc (Sen et al., 2011; Djelloul and Hamdaoui, 2014). Textile industries use more than 70% of the total produced dyes all over the world (Chudgar et al., 2014). Annually, these industries used a huge amount of water and about 5,000–10,000 tons of dyes which are released as effluent into the

waterways (Pirkarami and Olya, 2017; Yagub et al., 2014).

Most dyes are toxic to human beings and can cause allergy to skin, and act as mutagenic and carcinogenic agents (Khan and Malik, 2018; Lellis et al., 2019). Also can threaten aquatic organisms and can be resistant to natural biological degradation. Moreover, the presence of dyes in water bodies can decrease the transparency and light penetration through the water, related to the color, that influence photosynthesis then consequently reduces dissolved oxygen levels which affect aquatic biota (Sun et al., 2008; Hameed, 2009; Imran et al., 2015; Hassan and Carr, 2018). According to the molecule's ionic charge, dyes classified as anionic, cationic, and non-ionic. Methylene blue (MB) is a cationic dye that has numerous uses, includes dyeing cotton, wools, coating for paper stock, etc (Vargas et al., 2012; Fayoud et al., 2016). It can cause harmful effects to humans and animals such as eye burns, nausea, diarrhea, besides the negative effect on photosynthesis (El-Latif et al. 2010; Bulgariu et al., 2019). Therefore, the removal of such dyes from waste effluent is very important for the aquatic environment.

Numerous treatment techniques such as adsorption, ion exchange, reverse osmosis, biodegradation, coagulation-flocculation, electrochemical oxidation, fenton oxidation, and ozonation are applied to remove dyes from wastewater effluents (Pai et al., 2021). Adsorption is still the most efficient and cost-effective method for dye removal from waste effluent (Hassan and Carr, 2018).

Most of the recent dye removal studies have concentrated on the developing of locally low-cost agricultural and domestic waste materials or industrial by-products (Bello et al., 2015; Kadhom et al., 2020; Wong et al., 2020). For its availability in nature, clay minerals or its modifications, by calcination, treated with acid, salt exchange, and organification, have been used as effective sustainable and low-cost materials for the dyes removal from aqueous solution (El Mouzdahir

DOI: 10.21608/asejaiqsae.2021.186823

^{*}Department of Soil & Water Science,

Faculty of Desert and Environmental Agriculture,

Matrouh University, Egypt; E-Mails: ahmedelrefaey@alexu.edu.eg

Received June 10, 2021, Accepted, July 29, 2021.

et al., 2010; Pentrák et al., 2012; Liu et al, 2014; Medria et al., 2020). The variance in the dye adsorption capacity between different clay minerals is related to their surface properties and chemical structure. Bentonite, primarily smectite clay, has been successfully applied for adsorption of dyes for possessing permanent negative charges and exchangeable cations, its salt-resistance, and low hydration rate (Tahir and Rauf, 2006; Hong et al., 2009; Liu et al, 2014; Anirudhan and Ramachandran, 2015). Otherwise, cement kiln dust (CKD) is created in the cement manufacturing process as a by-product. Because of its physicochemical properties, CKD has reported as effective in removing heavy metals ions (Salem et al., 2015, El-Refaey, 2016 and 2017; El-Refaey and Mohammad, 2019) and dyes (Magdy and Altaher, 2018).

The aim of this study was to compare bentonite as a clay mineral and cement kiln dust as an industrial by-product for methylene blue dye removal from aqueous solutions. Bentonite and cement kiln dust characterization were compared. Moreover, their surface morphology and infrared Fourier transform (FTIR) were inspected before and after the experiment with MB dye adsorption. Batch experiments were conducted for evaluating the impact of different conditions, such as contact time, pH solution, adsorbent dosage, initial dye concentration, and temperature on MB dye removal. Kinetic studies were examined by pseudo-first-order, pseudo-second-order, and Elovich models, while the equilibrium results were examined by Langmuir and Freundlich isotherm models. Finally, to assess the feasibility and spontaneity of the removal reactions, thermodynamic parameters were determined.

MATERIALS AND METHODS

Adsorbate

The methylene blue (MB) is a basic dye has strong ability for adsorption onto solids. The Chemical structure of MB is $C_{16}H_{18} Cl N_3S$ (Fig. 1), and the maximum wavelength (λ_{max}) is 665 nm (Merck, German). One gram of MB dye was dissolved in 1000 mL distilled water to make a stock solution of 1000 mg/L. The different concentration solutions used in this study were 50, 100, 200, and 300 mg/L as prepared by dilution using distilled water.

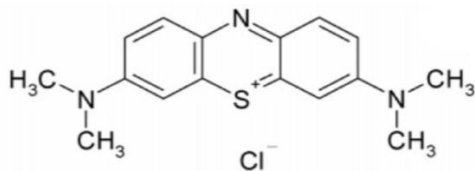


Fig.1. Chemical structure of methylene blue dye.

Adsorbents characterization

Two adsorbent materials were used in this study. (i) Bentonite (Bent) obtained from Egypt Company for Mining and Drilling Chemicals, (ii) cement kiln dust (CKD) collected from the El-Amerya cement plant, Alexandria, Egypt. Bentonite and CKD samples were sieved to ensure that the particle size range is less than 0.5 mm and then stored in plastic bottles for experimental uses.

X-ray diffraction (XRD) was conducted for bentonite and CKD by X-ray Powder Diffraction -XRD-D2 Phaser Bruker (Germany) using the $Cu K\alpha$ radiation ($\lambda=1.541 \text{ \AA}$) at 30 kV and 10 mA. The diffractogram was scanned from (2θ) 5 to 45° .

The elemental chemical composition of bentonite and CKD was identified by X-ray fluorescence spectroscopy (XRF) using Axios advanced sequential wavelength dispersive X-ray fluorescence Spectrometer (Malvern Panalytica) (Table.1).

The specific surface area of bentonite and CKD was estimated using Brunauer–Emmett–Teller (BET) method from N_2 -adsorption isotherms using a gas adsorption analyzer (Beckman Coulter SA(TM) 3100). The Barrett–Joyner–Halenda (BJH) method from the N_2 desorption isotherms was conducted for estimation of the pore size distribution (Nader, 2015).

Fourier transform-infrared (FTIR) spectra were determined at the range $400 - 4,000 \text{ cm}^{-1}$ by a Fourier transform infrared spectrometer (Infra-Red Bruker Tensor 37, German) using the KBr pellet method. FTIR spectra were conducted before and after MB dye adsorption experiments by the two sorbents.

The surface morphology of bentonite and CKD were performed by a Jeol IT-200 scanning electron microscope. Before the examination, samples provided with a thin layer of gold in the sputter-coating unit (JFC-1100E). Scanning electron microscopy (SEM) images were obtained at various magnification scales before and after adsorption experiments.

Adsorption experiments and analytical methods

Batch studies were conducted to study the influence of two adsorbents (Bent and CKD) on the removal of MB dye from aqueous solutions under different conditions. These conditions included: adsorbent doses (0.05, 0.1, 0.2, 0.4, 0.6, and 1 g); pre-adjusted pH values (4, 6, 8, 10, and 12); initial MB concentrations (50, 100, 200, 300 mg/L); NaCl concentrations (0.05, 0.1, 0.2, 0.3, 0.4 and 0.5 g); and different temperatures (25, 35, and 45°C). The pH values were adjusted using 1M NaOH or 0.1M HCl. For pH, NaCl concentrations, and various temperatures conditions, a 0.20 g of adsorbent was added to 40 ml (100 mg MB/L) in 50 mL plastic

centrifuge tubes, and agitation was carried out for 4 h which is sufficient. The supernatants were chemically analyzed for the determination of the residual MB concentration at the end of the equilibrium period. All of the experiments were replicated.

For Kinetic and isotherms studies, a 1.00g of sorbent was added to 250 mL glass Erlenmeyer flasks containing 200 mL of MB dye solution with various primary concentrations (50–300 mg/L) that were subjected to stirring at 130 rpm for 360 min at 25°C to reach equilibrium. Samples of the mixture solution were withdrawn at various intervals time, centrifuged and analyzed for MB dye concentration.

Standard concentrations of MB dye solution with the yield absorbance were obtained at 665 nm wavelength by using UV-VIS double beam JENWAY 140 spectrophotometer model 6850 for obtaining the calibration curve. The concentration of MB dye was determined in the supernatant after centrifuged (for 5 min at 5000 rpm) and measured for residual MB dye concentration. The adsorption amount (q_t) and the removal percentage of MB (R %) are calculated by the following equations:

$$q_t = (c_0 - c_t)V / m \quad (1)$$

$$R\% = (c_0 - c_t) / c_0 \times 100 \quad (2)$$

Where; q_t equals the amount of MB dye adsorbed amount at time t (mg/g), R equals the removal percentage (%), m is the CKD sample weight (g), V is the solution volume (dm^3), and c_0 and c_e equal the initial and equilibrium concentrations of MB dye, respectively.

RESULTS AND DISCUSSION

Adsorbents Characterization

X-ray diffraction and fluorescence analysis

The XRD diffractograms of bentonite and CKD are presented in Fig. (2). The XRD pattern indicated that montmorillonite is the main dominant mineral for natural bentonite. The XRD pattern also indicated the presence of quartz, dolomite, and calcite as impurities. Obviously, Calcite was the main mineral in CKD composition with miners of dolomite, feldspars, and quartz (Fig. 2).

The main compositions of bentonite and CKD as identified by X-ray fluorescence spectroscopy (XRF) are presented in Table (1). The oxides: SiO_2 (49.17%) and Al_2O_3 (14.55%) in bentonite are the main compositions with association other oxides present such as Fe_2O_3 and MgO which their percentages were higher than those of the CKD contents (Table 1).

Table 1. The main chemical constituents of bentonite (Bent) and cement kiln dust (CKD).

	Main Constituents (wt %)									
	SiO_2	Al_2O_3	Fe_2O_3	MgO	CaO	Na_2O	K_2O	SO_3	Cl	LOI*
Bent	49.17	14.55	7.37	2.23	0.75	3.25	0.68	0.31	0.85	17.96
CKD	11.10	3.08	2.07	1.82	43.42	4.93	1.41	10.99	2.63	37.4

*Loss on ignition

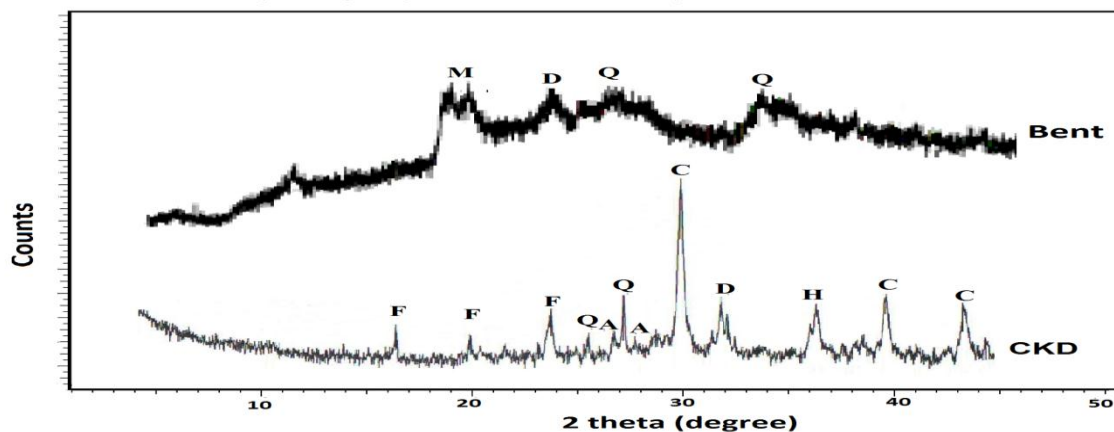


Fig.2. X-ray diffraction pattern of bentonite (Bent) and cement kiln dust (CKD).

(A: Anhydrite; C: Calcite, D: Dolomite; F: Feldspars; M: Montmorillonite; Q: Quartz).

These constituents are accountable for the removal of MB dye (Tahir and Rauf, 2006). On the other hand, CaO (43.42%) is the main component of CKD with some alkali oxides (sodium and potassium) as reported in many studies (El-Refaey, 2016; El-Refaey, 2017). Also, the percentages of SO₃ and Cl in CKD were higher than in those of bentonite. The adsorption characteristics of CKD can be attributed to both the high content of CaO and a significant percentage of SO₃ (Miller and Azad, 2000; Magdy and Altaher, 2018).

Specific surface area and pore analysis

The specific surface area for bentonite and CKD was determined by the common N₂-BET method at 77 ± 1° K. Figure (3) showed the increase of the volume of adsorbed N₂ with the rising of relative pressures (P/P₀) for bentonite than CKD. Therefore, the estimated

specific surface area of bentonite and CKD were 44.78 and 20.98 m²g⁻¹, respectively.

The desorption BJH pore size distribution for bentonite and CKD are listed in Table (2). Most of the pore diameter ranges fall within the range of mesoporous and microporous structures for both adsorbents. In addition, the pore diameter <6 nm, which is related to micropores, was the highest percentage in comparison with to the rest ranges, and bentonite has a higher percentage (49.59%) than CKD (37.67%). Thus, about 50% of the BJH pore diameter in bentonite relates to micropores and that may be reflected in the adsorption capacity. Also, the total pore volume of bentonite (61.70 mm³g⁻¹) was higher than CKD (37.30 mm³g⁻¹) (Table 2). CKD characterization depends upon the chemical composition of raw materials, the plant configuration, and the preprocessing type (Rahman et al., 2011; El-Refaey and Mohammad).

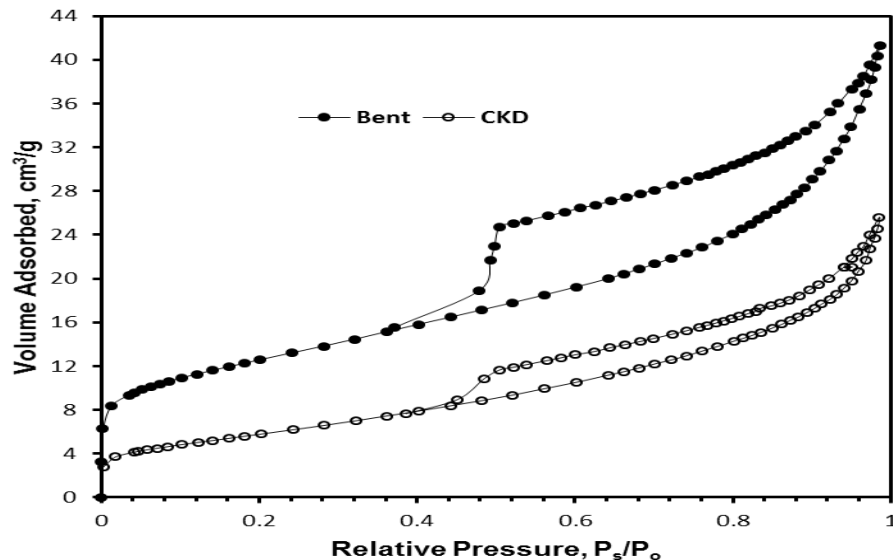


Fig. 3. N₂-adsorption isotherms of bentonite (Bent) and cement kiln dust(CKD).

Table 2. Desorption Barrett-Joyner-Halenda (BJH) pore size distribution for bentonite (Bent) and cement kiln dust (CKD).

Pore diameter range nm	Pore volume			
	Bent		CKD	
	ml g ⁻¹	%	ml g ⁻¹	%
< 6	0.0263	49.59	0.0136	37.67
6 - 8	0.0033	6.22	0.0028	7.68
8 - 10	0.0019	3.62	0.0019	4.40
10 - 12	0.0023	4.41	0.0020	4.74
12 - 16	0.0025	4.67	0.0018	5.07
16 - 20	0.0027	5.15	0.0022	6.02
20 - 80	0.0110	20.78	0.0096	26.55
> 80	0.0030	5.56	0.0028	7.88

FTIR analysis

FTIR spectra of the bentonite, as well as CKD, were conducted before and after the adsorption of MB dye from aqueous solutions including the bands corresponding to stretching and bending vibrations (Fig. 4). The bands at 3623.63 cm^{-1} and 916.36 cm^{-1} confirmed the presence of dioctahedral Smectite mineral with Al–OH–Al (Toor et al., 2015; Kumararaja et al., 2017). The band at 3695.61 cm^{-1} is assigned to Al–Mg–OH stretching and Al–Fe–OH bending vibration at 787.52 cm^{-1} was representative of the bentonite clays (Sikdar et al., 2008; Osman et al., 2017). Peaks position at 1032.23 cm^{-1} , 529.11 cm^{-1} and 465.85 cm^{-1} were attributed to the Si–O stretching vibration of bentonite mineral (Paluszkiwicz et al., 2008; Benhouria et al., 2015; Kumararaja et al., 2017). The band at 1463.20 cm^{-1} was corresponded to C–H stretching (Pavia et al., 2009; Anirudhan and Ramachandran, 2015). The broad band's at 3421.38 and 1633.03 cm^{-1} ascribed to the

stretching of O–H stretching vibrations in the mineral (Toor et al., 2015; Shehata et al., 2016; Reddy T et al., 2017). On the other hand, CKD FTIR spectrum indicated the presence of carbonate (CO_3^{2-} group) at 1424.60 cm^{-1} and 873.58 cm^{-1} (Salem and Velayi, 2012; El-Refaey, 2016 and 2017). Peaks position at 1133.04 cm^{-1} and 710.20 cm^{-1} attributed to silicate stretching vibration (Al-Ghouti, 2003; Saraya and Aboul-Fetouh, 2012). The bands at 2978.79 and 2872.79 cm^{-1} are attributed to C–H stretching in alkanes (Xue et al., 2007; Meziti and Boukerroui, 2012; Chinoune et al., 2016), but the wave number of 613.30 cm^{-1} is related to K–O vibration (Salem et al., 2012; El-Refaey and Mohammad, 2019). The existence of shifts and disappearance of functional group peaks in bentonite and CKD bands, were detected in FTIR spectrum after the adsorption experiment, which confirm the bending of MB dye onto bentonite and CKD (Fig.4).

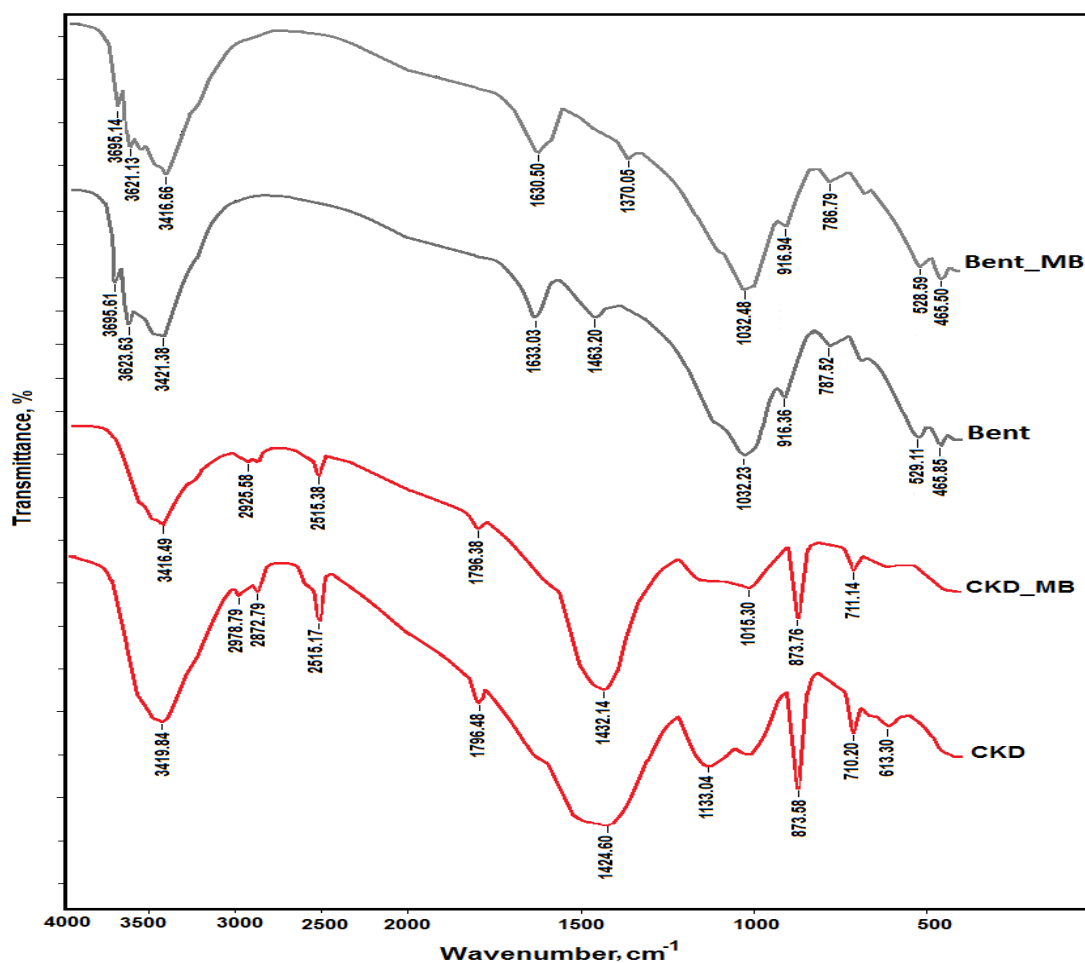


Fig. 4. FTIR spectra of bentonite (Bent) and cement kiln dust (CKD) before and after the methylene blue (MB) dye removal.

Scanning electron microscopy analysis

Bentonite and CKD surface morphology was analyzed by scanning electron microscopy (SEM) before and after the removal reaction of methylene blue (MB) dye removal (Fig.5). SEM image demonstrated that bentonite has a clear plate with lamellar curly surface morphology. While, SEM of CKD revealed irregular shape particles distributed heterogeneously. The difference in morphology between before and after MB removal reaction was clearly observed with CKD than with bentonite. Hence, CKD particles were concealed in bulk and complexes formation and it may denote different mechanisms for MB dye removals.

Removal of methylene blue

Influence of contact time and initial dye concentration

The influence of contact time and the initial concentration of MB dye on the adsorption processes by Bent and CKD are shown in Fig. (6). The results revealed that the MB dye removal was increased with time with rapid removal of MB dye in the first 60 min for bentonite and CKD at all tested initial MB

concentrations then slowed the removal down close to equilibrium. The first rapid removal percentage of MB may be ascribed to a large number of binding sites on the adsorbent surfaces, while the slower removal percentage may be occurred after the saturation of the binding sites before reaching the equilibrium (Hameed and Ahmad, 2009; Omer et al., 2018). For bentonite, there was increasing in MB removal percentage and reaching equilibrium time after 2 h for 50- 100 mg/L. But for MB dye concentration 200-300mg/L, 3 h was very sufficient (Fig. 6-a). For CKD, the MB dye removal was gradually increased with time till it reached equilibrium after 3h and maximum MB dye removal percentage for all initial concentrations. In general, the equilibrium time, a steady-state approximation, varied depending on various adsorbents and adsorption conditions (Hameed, 2009). Otherwise, the MB dye removal percentage decreases with increasing the concentration from 50 to 300 mg/L. For bentonite, MB dye removal percentage decreased from 92.55 to 42.14% (Fig. 6-a) and from 73.57 to 26.67% for CKD with increasing the initial MB concentration from 50 to 300 mg/L (Fig. 6b).

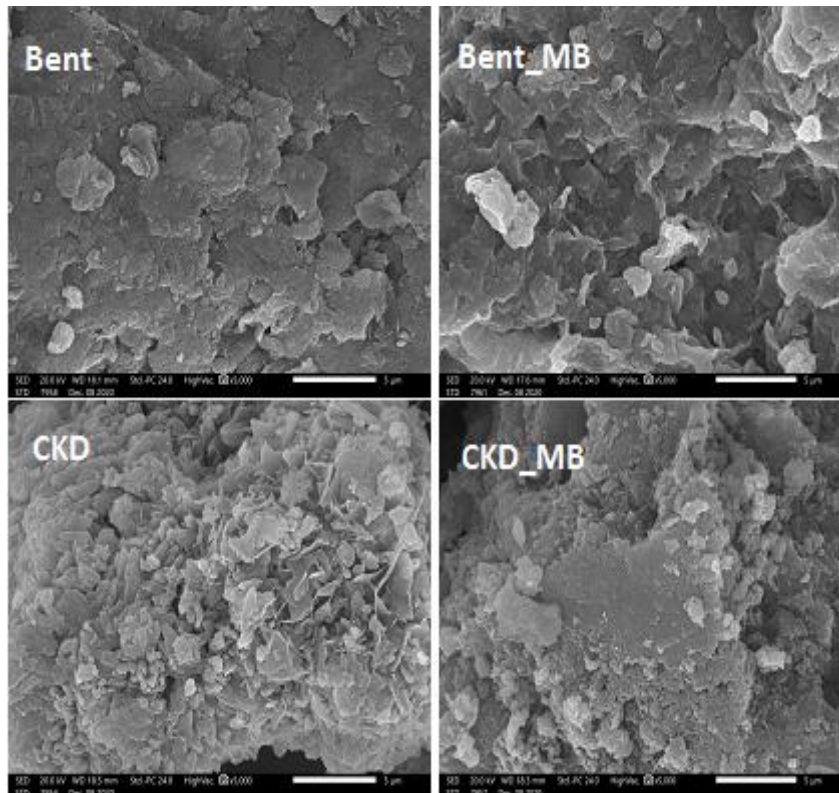


Fig. 5. SEM images analysis of bentonite (Bent) and cement kiln dust (CKD) before and after methylene blue (MB) dye removal reactions from aqueous solutions.

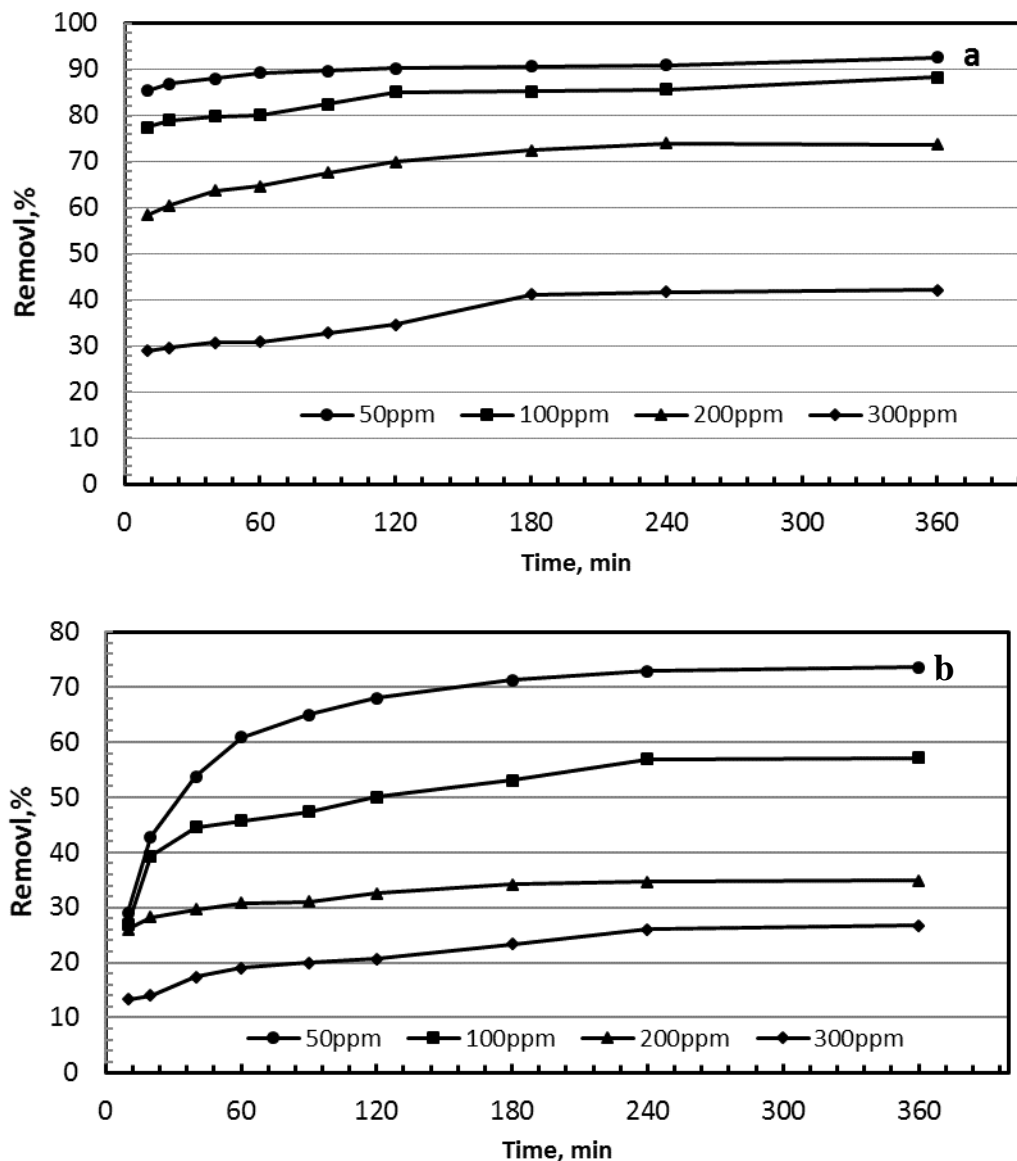


Fig. 6. Kinetic of methylene blue (MB) dye removal by bentonite (a) and cement kiln dust (b) at different initial dye concentrations (50 – 300 mg/L) at room temperature (25°C).

Influence of adsorbent dose

Generally, gradually increasing the adsorbent mass from 0.05 g to 1.0g (at 100 mgMB/L) showed an increase in the MB dye removal by bentonite (Fig. 7-a). The increase of removal percent was due to the increase in the adsorption surface sites. There were close results for bentonite (88.25%) and CKD (84.04%), at 1.0 g mass adsorbent. This decrease indicates the role of the ratio of adsorbent with a concentration of MB in the system.

Influence of pH

One of the affected parameters on the dye removal is the pH because of its effect on dye molecules ionization process and the adsorbent functional groups (Liu et al, 2014). Results reveal that the removal percentages of MB dye by bentonite and CKD increase with increasing solution pH from 4 to 12 (Fig. 6-b). At the initial low pH system, the numbers of surface negative charge sites are decreased, and the surface positive charge sites are

increased. As a result that the MB dye cation removal decreases because of electrostatic repulsion and the competing of excess H^+ ions with MB dye (Tahir and Rauf, 2006; Djelloul and Hamdaoui, 2014). For bentonite, the removal percentage increased from 45.00 to 81.29% with increasing pH from 4 to 6 and there were no significant differences in the removal percentage as the pH value was beyond 6.0. This could be explained as due to clay mineral buffering capacity (Grim, 1968; Bloom, 2000). So, bentonite could be used as an efficient removal sorbent for MB in a considerable pH range (6 -12). For clay minerals, the electric layer polarity change on both the silica and alumina contents from positive to negative charge, especially in the higher pH and that could increase the dye removal by appealing the dye cations (Tahir and Rauf, 2006; Anirudhan and Ramachandran, 2015; Abd-Elhamid et al., 2019).

Otherwise, the removals of MB dye by CKD slightly increasing with increasing from pH 4 to 8. However, a sharp rising in their removal percentage of MB dye by CKD (84.7%) at pH 12 revealed that the removal efficiency is considerable at the high alkane range.

Influence of salinity

Generally, NaCl is presented in the dyeing industries wastewaters, especially textile industries, for enhancing the fixation of dyes (Liu et al., 2014). So, the effect of salinity on the MB dye removal by bentonite and CKD was investigated in the range of 0.05- 0.5 g of NaCl (Fig. 7-c). Figure (7-c) showed that the MB dye removal percentage was increased as NaCl concentration in solution increased, to reach 98.82% for bentonite and 64.46% for CKD at 0.5g NaCl.

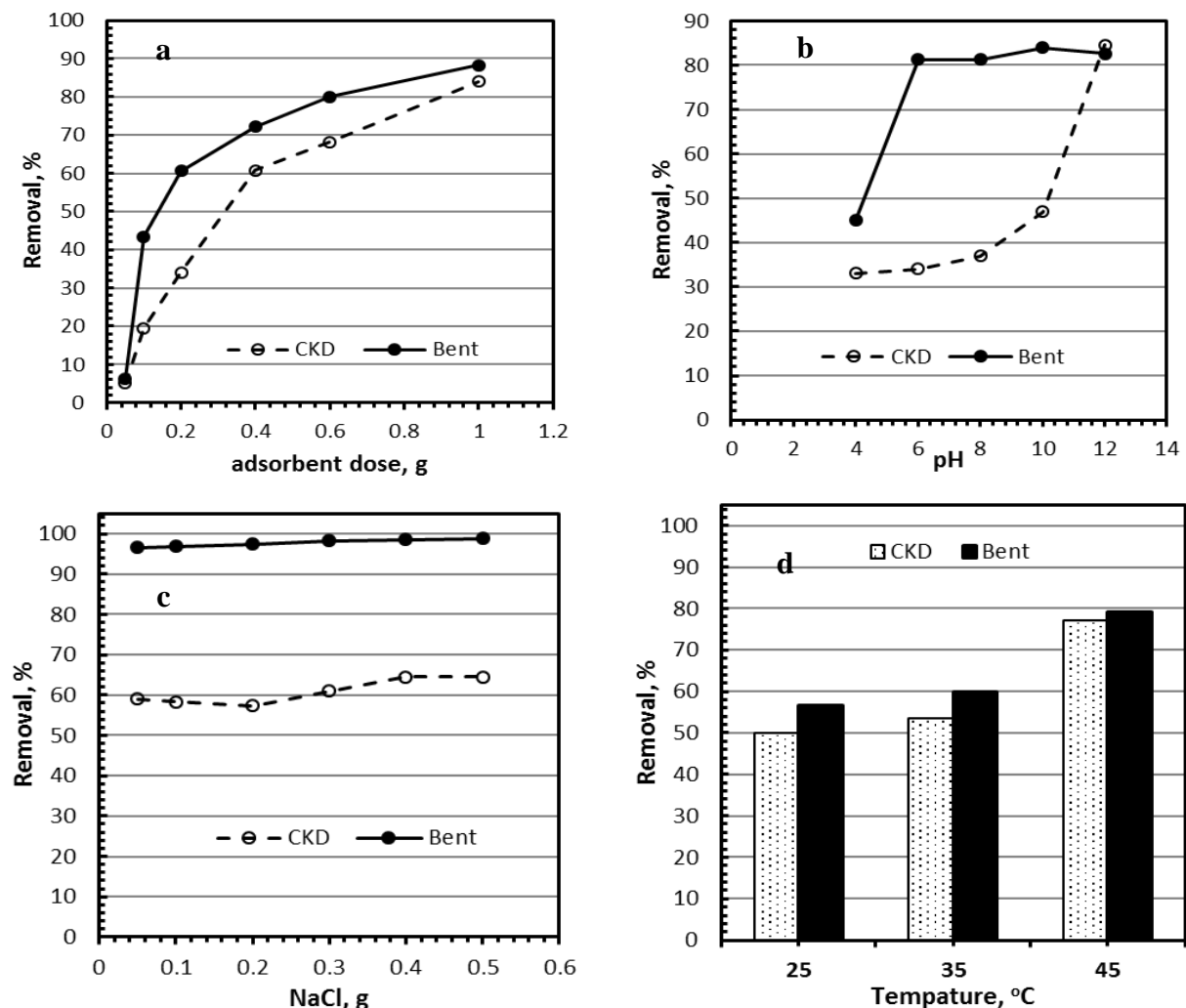


Fig. 7. Effect of adsorbent dose (a), pH (b), NaCl (c) and temperature (d) on the removal percentage of methylene blue (MB) dye by bentonite (Bent) and cement kiln dust (CKD).

That can be interpreted by the electrostatic force is repulsive with increasing Na^+ ion concentration (Alberghina et al., 2000; Oladipo et al., 2014). Also, increasing salt concentration, with the Cl^- existence, can affect the dissociation of MB dye molecules by supporting the protonation, and thus the detachment dye ions are encouraged to contact the surface of the adsorbent, toward increasing the capacity of adsorption (Vermohlen et al., 2000; Tekin et al., 2005; Al-Degs et al., 2008; Liu et al., 2014). Clearly, the results indicated that the increase of NaCl concentration showed a higher progressive effect on the performance of the removal of MB dye by bentonite (98.82%) than CKD (64.46%) at 0.5g NaCl.

Influence of temperature

The effect of different temperatures (25, 35, and 45°C) on MB dye removal onto bentonite and CKD is illustrated in Fig. (7-d). The obtained results indicated the increasing percentage of MB dye removal with increasing the solution temperature for both adsorbents. Xue et al. (2007) and Toor et al. (2015) reported that increasing the temperature could result in deeper penetration of protons into clay layers and the removal of hydrated water provides further adsorption sites and increasing the specific surface area. On other hand, at low temperatures, the water molecules adsorption is higher than that of dye molecules due to their competition in the clay inter-lamellar spaces (Omer et al., 2018).

Kinetic studies

Different kinetics models were conducted to understand and describe the removal of MB dye by bentonite and CKD. These models are fractional power (Ho and McKay, 2002), Elovich (Inyang et al., 2016), pseudo-first-order (Lagergren, 1898), pseudo-second-order (Ho, 2006), and intra-particle diffusion (Medria et al., 2020) models. The linear form of the used models:

$$\text{Fractional power: } \ln q_t = \ln a + b \ln t \quad (3)$$

$$\text{Elovich: } q_t = \frac{1}{\beta} \ln(\alpha\beta) + \frac{1}{\beta} \ln t \quad (4)$$

Pseudo-first-order:

$$\log(q_e - q_t) = \log q_e - k_1 t / 2.303 \quad (5)$$

Pseudo-second order:

$$\frac{t}{q_t} = 1/k_2 q_e^2 + t/q_e \quad (6)$$

$$\text{Intra-particle diffusion: } q_t = k_i t^{1/2} + C \quad (7)$$

Where;

q_e and q_t equal the MB dye adsorbed (mg g^{-1}) by bentonite or by CKD at equilibrium and at a time t , respectively; α equals primary adsorption coefficient

(mg/g min^{-1}); β equals desorption coefficient (g mg^{-1}); k_1 and k_2 equal the rate constants of pseudo-first (min^{-1}) and second-order models ($\text{g} \cdot \text{mg}^{-1} \text{min}^{-1}$), respectively; k_i ($\text{gmg}^{-1} \text{min}^{-1/2}$) equals intra-particle diffusion rate constant; C equals constant (mg g^{-1}) that provides evidence of the boundary layer thickness.

The removal kinetic parameters of different concentrations (50-300 mgMB/L) onto bentonite and CKD are shown in Table (3). The obtained data for both adsorbents pointed out a good agreement with the second-order equation for all examined initial dye concentrations. For most of the initially tested concentrations of MB dye, the regression coefficients (R^2) for the two adsorbents regarding pseudo-second order model were more than 0.99 (Table 3). The excellent agreement of the obtained data to pseudo-second-order equation and independent of the rate constants values from initial MB dye concentration indicated the chemical nature of the adsorption process (Fig. 8) (Wu et al., 2009; Anirudhan and Ramachandran, 2015; Konggudinata et al., 2017; Magdy and Altaher, 2018).

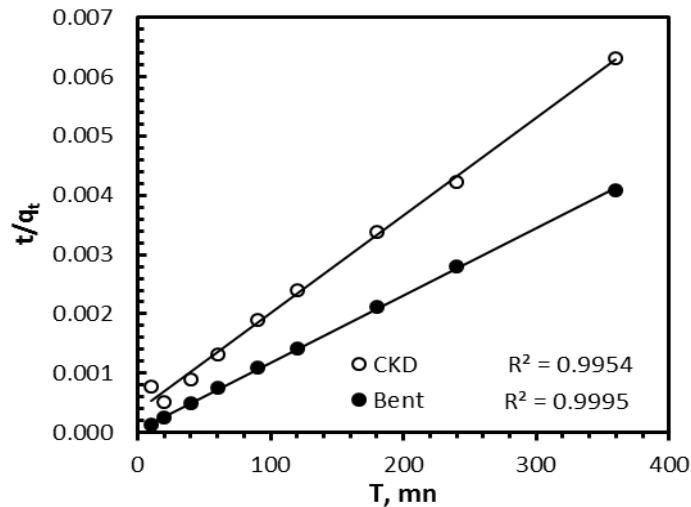
Under aqueous conditions, the surface negative charged functional groups drive the adsorption of dye molecules into adsorbents. However, this can be assigned mainly to be through the ion exchange process (Hassan and Carr, 2018). For bentonite, montmorillonite as the main content has a net surface negative charge due to isomorphous substitutions on its structure and compensates with interlayer cations that can be replaced by MB cations (Zhu et al., 2009; Şahin et al., 2015). Swelling may be having a significant role in increasing its inner specific surface area and pore size (Li et al., 2019). Also, metal oxides and hydroxides in the adsorbent surfaces could form complexes with dye in an aqueous solution (Netpradit, et al., 2003). However, the adsorption of MB dye by bentonite and CKD could take place through different stages. In the beginning, the dye molecules move to form a thin layer surrounding the hydrated adsorbent, and then the dye particles diffuse through the thin hydration shell around the adsorbent. After that the dye particles penetrate into the adsorbent surface through the pores, finally, it is adsorbed on the adsorbent surfaces (Tahir and Rauf, 2006; Fierro et al., 2008; Magdy and Altaher, 2018).

Adsorption isotherm studies

The isotherm analysis gives an idea of how the adsorbent will relate to the adsorbent and its adsorption capacity (Salleh et al., 2011). The results of the isotherms experiments were analyzed using Freundlich (Freundlich, 1906), Langmuir (Langmuir, 1918),

Table 3. Kinetic parameters for the removal of methylene blue (MB) dye onto bentonite and cement kiln dust (CKD).

model	Bentonite				CKD			
	50mg/L	100mg/L	200mg/L	300mg/L	50mg/L	100mg/L	200mg/L	300mg/L
Fractional power								
a	40531.96	70260.17	97713.20	61033.30	3575.39	10500.53	43432.99	23892.09
b	0.200	0.036	0.072	0.119	0.453	0.321	0.084	0.207
R ²	0.984	0.933	0.976	0.847	0.664	0.672	0.981	0.981
Elovich								
α	1.063x10 ¹⁹	2.924 x10 ¹³	1.48 x10 ⁸	6.53 x10 ⁵	3743.57	10665.20	5406.36	5406.36
β	0.0010778	0.000331	0.0001039	0.00008	0.00012	0.000094	0.000195	0.000084
R ²	0.8733	0.928	0.972	0.824	0.853	0.853	0.981	0.964
Pseudo-first-order								
q _e	3127.99	10646.44	37317.78	68927.64	25032.41	27207.36	27346.73	39849.20
k ₁	-0.00331	-0.0067	-0.0134	-0.01543	-0.01982	-0.00501	-0.01511	-0.00873
R ²	0.905	0.899	0.942	0.973	0.965	0.839	0.942	0.97315
Pseudo-second-order								
q _e	45454.55	90909.09	142857.14	125000	41666.66	62500.00	71428.57	83333.33
K ₂	0.000002	0.000002	0.0000011	0.0000005	0.0000007	0.0000007	0.0000018	0.0000005
R ²	0.999	0.999	0.999	0.994	0.980	0.995	0.999	0.992
Intra-particle diffusion								
k _i	200.90	686.70	2110.40	2981.69	1590.00	2082.40	1112.70	2674.20
C	42652	75666	113316	74453	12849	24384	51536	33360
R ²	0.913	0.655	0.925	0.913	0.652	0.6555	0.915	0.966

**Fig. 8. Pseudo-second-order plots for methylene blue (MB) dye (at 100mgMB/L) removal kinetics by bentonite (Bent) and cement kiln dust (CKD)**

and Temkin (El-Refaey and Mohammad, 2019) isotherm models as follows:

$$\text{Freundlich: } q_e = K_F C_e^{1/n} \quad (8)$$

$$\text{Langmuir: } q_e = q_{\max} (K_L C_e / (1 + K_L C_e)) \quad (9)$$

$$\text{Temkin: } \theta = RT/\Delta Q \ln K_0 C_e \quad (10)$$

Where:

q_e: MB dye adsorbed (mg g⁻¹), C_e: equilibrium concentration of MB dye (mg L⁻¹), K_F: constant associated with the adsorption capacity (mg^{1-(1/n)} L^{1/n}g⁻¹), n: a constant, q_{max}: maximum adsorption capacity (mg g⁻¹), K_L: constant associated with the adsorption free energy (L mg⁻¹), θ: fractional coverage, R: universal gas coefficient (kJ mol⁻¹ K⁻¹), T:

temperature ($^{\circ}\text{K}$), ΔQ : ($-\Delta H$) adsorption energy difference (kJ mol^{-1}), and K_0 : Temkin coefficient (L mg^{-1}).

The isotherm parameters of methylene blue (MB) dye removed by bentonite (Bent) and CKD are shown in Table (4). The results were fitted within the following isotherms order: Langmuir>Freundlich>Temkin according to regression coefficients values (R^2) for both adsorbents (Table.4). The equilibrium was excellently fitted to Langmuir isotherm and R^2 for bentonite and CKD were 0.994 and 0.996, respectively (Fig.9). The Langmuir isotherm was established to represent the chemisorption. According to Langmuir model theory, the sorption is confined in a mono-layer, nointeraction among the MB dye particles, and no additional adsorption occurred on a site after a dye molecule has occupied this site (Wang and Ariyanto, 2007; Liu et al., 2014). The maximum sorption capacity of bentonite for MB dye ($3257.33 \text{ mg g}^{-1}$) was significantly higher than that of CKD ($2150.54 \text{ mg g}^{-1}$) (Table.4). The presented result that the adsorbent used in this study indicated higher adsorption capacity as compared to those prepared from agricultural waste (Kadhom et al., 2020), ion-exchange resin adsorbents (Hassan and Carr, 2018), and activated carbon derived from any carbonaceous raw material (Katheresan et al., 2018).

Thermodynamic studies

Thermodynamic parameters of MB dye removal onto bentonite and CKD surfaces were determined using van't Hoff relation in the range of temperature was 298–318 $^{\circ}\text{K}$. The following equations used for the estimation of Gibbs free energy (ΔG°), enthalpy change (ΔH°), and

the entropy change (ΔS°) parameters (Trana et al., 2016; El-Refaey, 2017, Danish et al., 2018):

$$\Delta G^{\circ} = -RT \ln K_L \quad (12)$$

$$\Delta G^{\circ} = \Delta H^{\circ} - T \Delta S^{\circ} \quad (13)$$

$$\ln K_L = -\frac{\Delta G^{\circ}}{RT} = -\frac{\Delta H^{\circ}}{RT} + \frac{\Delta S^{\circ}}{R} \quad (14)$$

Where:

R: gas coefficient (8.314 J/mol K), K_L : equilibrium constant obtained by divided MB adsorbed dye ($q_e, \text{ mg g}^{-1}$) by the equilibrium concentration of MB dye ($C_e, \text{ mg L}^{-1}$) and T: absolute temperature ($^{\circ}\text{K}$).

The determined thermodynamic values of Gibbs free energy change (ΔG°), enthalpy (ΔH°), and entropy (ΔS°) are shown in Table (5). The negative values of ΔG° for removal of MB dye by bentonite and CKD indicate that the adsorption is spontaneous and the feasibility of the process for both sorbents (Table 5). The decrease of ΔG° values for the MB dye removal by bentonite and CKD with increasing temperature gives an increase in the process feasibility and becomes more favorable at higher temperatures. The ΔH° positive value for bentonite pointed out that the nature of the adsorption process is endothermic. Spontaneous and endothermic adsorptions have also been described by Hong et al. (2009), Chinoune et al. 2016, and Omer et al. (2018) for bentonite, and Kadhim and Hassan (2016) for CKD. The positive value of ΔS° reflects the affinity of bentonite and CKD for removing MB dye and suggests growing the randomness at the solid/solution interface through the removal reactions.

Table 4. Adsorption isotherm parameters of methylene blue (MB) dye by bentonite (Bent) and cement kiln dust (CKD).

	Freundlich			Langmuir			Temkin		
	K_F $\text{mg}^{1-(1/n)} \text{L}^{1/n} \text{g}^{-1}$	1/n	R^2	q_m mg g^{-1}	K_L Lmg^{-1}	R^2	A L g^{-1}	B	R^2
Bent	972.71	0.271	0.785	3257.33	0.031	0.994	3.218	580.9	0.771
CKD	481.32	0.268	0.973	2150.54	0.046	0.996	0.96	371.09	0.991

Table 5. Thermodynamic parameters of methylene blue (MB) dye removal by bentonite (Bent) and cement kiln dust (CKD) from aqueous solutions at temperature range from 298 to 323 ± 2 $^{\circ}\text{K}$.

	$\Delta G^{\circ}, \text{kJ/mol}$			ΔS°	ΔH°
	298K	308K	323K	J/mol K	kJ/mol
Bent	-13.66	-14.57	-16.93	2.34	0.50
CKD	-13.23	-13.79	-16.79	2.53	0.57

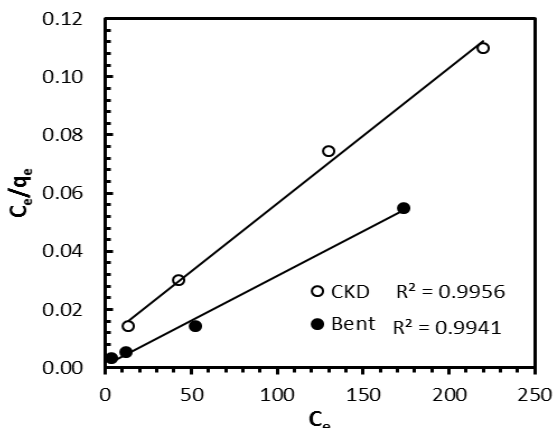


Fig. 9. Methylene blue (MB) dye adsorption isotherm regression using the Langmuir equation for bentonite (Bent) and cement kiln dust (CKD)

CONCLUSION

The chemical composition and surface characteristics of bentonite and cement kiln dust were investigated by XRF, XRD, BET specific surface area, FTIR, and SEM analysis. The results of batch experiments indicated that the methylene blue (MB) dye removal has been increased with time and decreased as its initial concentration increased. On the other hand, increasing the dose of adsorbent increased the dye removal percentage by both adsorbents. The removal of MB dyes onto bentonite was slightly pH dependent at $pH > 6$ with a maximum removal percent of 81.29% at pH 12. Otherwise, the removal percent of MB dye by CKD increased with pH increase to reach its maximum (84.7%) at pH 12. The bentonite adsorption capacity was also increased by the presence of NaCl compared to CKD. Langmuir isotherm was a preferable fit for the experimental results for both adsorbents. The maximum adsorption capacity for bentonite and CKD were $3257.33 \text{ mg g}^{-1}$ and $2150.54 \text{ mg g}^{-1}$, respectively. Kinetic data for MB dye removal by bentonite and CKD obeyed the pseudo-second-order at all tested concentrations. The high removal of MB dye indicated a high potential for the two adsorbents. For economic issues, CKD proved to be effective and to be applied for removing MB dye from wastewater at the same time; it is considered a value-added product valuable for hazardous waste disposal in waterways.

ACKNOWLEDGE

The author thanks Dr. Mohamed A. Osman for his cooperation in XRD identification.

REFERENCES

- Abd-Elhamid, A. I., F. E. Gomaa, A. A. Magda. 2019. Methylene Blue and Crystal Violet Dyes Removal (As A Binary System) from Aqueous Solution Using Local Soil Clay: Kinetics Study and Equilibrium Isotherms. *Egypt. J. Chem.* 62(3): 941- 954.
<https://doi.org/10.21608/EJCHEM.2018.4113.1360>
- Alberghina G., R. Bianchini, M. Fichera, S. Fisichella. 2000. Dimerization of cibacron blue F3GA and other dyes: influence of salts and temperature. *Dyes Pigm.*46:129–37.
[https://doi.org/10.1016/S0143-7208\(00\)00045-0](https://doi.org/10.1016/S0143-7208(00)00045-0)
- Al-Degs Y.S., M.I. El-Barghouthi, A.H. El-Sheikh, G.M. Walker. 2008. Effect of solution pH, ionic strength, and temperature on adsorption behavior of reactive dyes on activated carbon. *Dyes Pigm.*77: 16– 23.
<https://doi.org/10.1016/j.dyepig.2007.03.001>
- Al-Ghouti, M. A., M. A. M. Khraisheh, S. J. Allen, M. N. Ahmad. 2003. The removal of dyes from textile wastewater: a study of the physical characteristics and adsorption mechanisms of diatomaceous earth. *J. Environ. Manage.* 69: 229–238.
<https://doi.org/10.1016/j.jenvman.2003.09.005>
- Anirudhan, T.S., M. Ramachandran. 2015. Adsorptive removal of basic dyes from aqueous solutions by surfactant modified bentonite clay (organoclay): Kinetic and competitive adsorption isotherm. *Process Saf. Environ. Prot.* 95:215–225.
<https://doi.org/10.1016/j.psep.2015.03.003>
- Bello, O.S., K.A. Adegoke, , A.A. Olaniyan, H. Abdulazeez. 2015. Dye adsorption using biomass wastes and natural adsorbents: overview and future prospects. *Desalin. Water Treat.* 53: 1292–1315.
<https://doi.org/10.1080/19443994.2013.862028>
- Benhouria, A., M.A. Islam, H. Zaghoulane-Boudiaf, M. Boutahala, B.H. Hameed. 2015. Calcium alginate-bentonite-activated carbon composite beads as highly effective adsorbent for methylene blue. *Chem. Eng. J.* 270: 621–630. <https://doi.org/10.1016/j.cej.2015.02.030>
- Bloom, P.R. 2000. Soil pH and pH buffering. In Sumner: M.E., (ed.). *Handbook of Soil Science* CRC Press. USA.pp. 333-352
- Bulgariu, L., L.B. Escudero, O.S. Bello, M. Iqbal, J. Nisar, K.A. Adegoke, F. Alakhras, M. Kornaros, I., Anastopoulos. 2019. The utilization of leaf-based adsorbents for dyes removal: A review. *J. Mol. Liq.* 276: 728–747. <https://doi.org/10.1016/j.molliq.2018.12.001>
- Chinoune, K., K. Bentalab, Z. Bouberka, A. Nadim, U. Maschke. 2016. Adsorption of reactive dyes from aqueous solution by dirty bentonite. *Appl. Clay Sci.* 123: 64–75. <https://doi.org/10.1016/j.clay.2016.01.006>
- Chudgar, R.J., J. Oakes. 2014. Dyes, azo. In: Kirk-Othmer *Encycl. Chem. Technol.* Hoboken NJ, USA: John Wiley & Sons, Inc.

- Danish, M., T. Ahmad, S. Majeed, M. Ahmad, L. Ziyang, Z. Pin, S. M. Shakeel Iqbal. 2018. Use of banana trunk waste as activated carbon in scavenging methylene blue dye: Kinetic, thermodynamic, and isotherm studies. *Bioresour. Technol. Reports* 3: 127–137. <https://doi.org/10.1016/j.biteb.2018.07.007>
- Djelloul, C., O. Hamdaoui. 2014. Removal of cationic dye from aqueous solution using melon peel as nonconventional low-cost sorbent. *Desalin. Water Treat.* 52: 7701–7710. <https://doi.org/10.1080/19443994.2013.833555>
- El Mouzdahir, Y. A. Elmchaouri, R. Mahboub, A. Gil, S. A. Korili. 2010. Equilibrium modeling for the adsorption of methylene blue from aqueous solutions on activated clay minerals, *Desalination*. 250: 335–338. <https://doi.org/10.1016/j.desal.2009.09.052>
- El-Latif, M.M.A., A. M. Ibrahim, M. F. El-Kady. 2010. Adsorption equilibrium, kinetics and thermodynamics of methylene blue from aqueous solutions using biopolymer oak sawdust composite. *J. Am. Sci.* 6: 267–283.
- El-Refaey, A.A. 2016. Comparative performance of cement kiln dust and activated carbon in removal of cadmium from aqueous solutions. *Water Sci. Technol.* 73. <https://doi.org/10.2166/wst.2015.651>
- El-Refaey, A.A. 2017. Investigation of copper removal from aqueous solution by cement kiln dust as industrial by-product, *Alexandria Sci. Exch. J.*, 38: 149–158. <https://doi.org/10.21608/ASEJAIQJSAE.2017.2455>
- El-Refaey, A.A., S.G.Mohamed. 2019. Removal of lead from aqueous solutions using cantaloupe peels as a biosorbent vs. cement kiln dust as an industrial by-product. *Desalin. Water Treat.* 166: 62–71. <https://doi.org/10.5004/dwt.2019.24626>
- Fayoud, N., S. Tahiri, S. Alami Younssi, A. Albizane, D. Gallart-Mateu, M. L. Cervera, M. de la Guardia. 2016. Kinetic, isotherm and thermodynamic studies of the adsorption of methylene blue dye onto agro-based cellulosic materials. *Desalin. Water Treat.* 57:16611–16625. <https://doi.org/10.1080/19443994.2015.1079249>
- Fierro, V., V. Torné-Fernández, D. Montané, A. Celzard. 2008. Adsorption of phenol onto activated carbons having different textural and surface properties, *Microporous Mesoporous Mat.* 111: 276–284. <http://dx.doi.org/10.1016/j.micromeso.2007.08.002>
- Freundlich, H. M. F. 1906. Over the adsorption in solution, *J. Phys. Chem.* 57: 385–471
- Grim, R. E. 1968. *Clay mineralogy*, 2nd ed. McGraw-Hill, New York.
- Hameed, B.H. 2009. Grass waste: A novel sorbent for the removal of basic dye from aqueous solution. *J. Hazard. Mater.* 166: 233–238. <https://doi.org/10.1016/j.jhazmat.2008.11.019>
- Hameed, B.H., A. A. Ahmad. 2009. Batch adsorption of methylene blue from aqueous solution by garlic peel, an agricultural waste biomass. *J. Hazard. Mater.* 164: 870–875. <https://doi.org/10.1016/j.jhazmat.2008.08.084>
- Hassan, M.M., C. M. Carr. 2018. A critical review on recent advancements of the removal of reactive dyes from dyehouse effluent by ion-exchange adsorbents. *Chemosphere*. 209: 201–219. <https://doi.org/10.1016/j.chemosphere.2018.06.043>
- Ho, Y. S. 2006. Second-order kinetic model for the sorption of cadmium onto tree fern: a comparison of linear and nonlinear methods. *Water Res.* 40 (1): 119–125. <https://doi.org/10.1016/j.watres.2005.10.040>
- Ho, Y. S., G. McKay. 2002. Application of kinetic models to the sorption of copper (II) on to peat. *Adsorp. Sci Technol.* 20 (8): 797–815. <https://doi.org/10.1260/026361702321104282>
- Hong, S., C. Wen, J. He, F. Gan, Y. S. Ho. 2009. Adsorption thermodynamics of Methylene Blue onto bentonite. *J. Hazard. Mater.* 167:630–633. <https://doi.org/10.1016/j.jhazmat.2009.01.014>
- Imran, M., D. E. Crowley, A. Khalid, S. Hussain, M.W. Mumtaz, M. Arshad. 2015. Microbial biotechnology for decolorization of textile wastewaters. *Rev. Environ. Sci. Biotechnol.* 14: 73–92. <https://doi.org/10.1007/s11157-014-9344-4>
- Inyang, H. I., A. Onwawoma, S. Bae. 2016. The Elovich equation as a predictor of lead and cadmium sorption rates on contaminant barrier minerals. *Soil Tillage Res.* 155: 124 – 132. <https://doi.org/10.1016/j.still.2015.07.013>
- Kadhim, D.A., S. A. Hassan. 2016. The performance of Cement Kiln Dust in Removal of Some Dyes from Aqueous Solutions. *Am. J. Pharm Tech Res.* 6:298-324.
- Kadhom, M., N. Albayati, H. Alalwan, M. Al-Furaiji. 2020. Removal of dyes by agricultural waste. *Sustain. Chem. Pharm.* 16:100259. <https://doi.org/10.1016/j.scp.2020.100259>
- Katheresan, V., J. Kansedo, S. Y. Lau. 2018. Efficiency of various recent wastewater dye removal methods: A review. *J. Environ. Chem. Eng.* 6: 4676–4697. <https://doi.org/10.1016/j.jece.2018.06.060>
- Khan, S., A. Malik. 2018. Toxicity evaluation of textile effluents and role of native soil bacterium in biodegradation of a textile dye. *Environ Sci Pollut Res Int.* 25(5): 4446-4458. <https://doi.org/10.1007/s11356-017-0783-7>
- Konggidinata, M.I., B. Chao, Q. Lian, R. Subramaniam, M. Zappi, D.D. Gang. 2017. Equilibrium, kinetic and thermodynamic studies for adsorption of BTEX onto Ordered Mesoporous Carbon (OMC). *J. Hazard. Mater.* 336: 249–259. <https://doi.org/10.1016/j.jhazmat.2017.04.073>
- Kumararaja, P., K. M. Manjaiaha, S. C. Datta, B. Sarkar. 2017. Remediation of metal contaminated soil by aluminium pillared bentonite: Synthesis, characterisation, equilibrium study and plant growth experiment. *Appl. Clay Sci.* 137: 115–122. <https://doi.org/10.1016/j.clay.2016.12.017>

- Lagergren, S., 1898. About the theory of so-called adsorption of soluble substances. *Kungliga Svenska Vetenskapsakademiens* 24 (4):1–39.
- Langmuir, S. 1918. The adsorption of gases on plane surfaces of glass, mica and platinum. *J. Am. Chem. Soc.* 40 (9): 1361–1403. <https://doi.org/10.1021/ja02242a004>
- Lellis, B., C.Z. Fávaro-Polonio, J.A. Pamphile, J. C. Polonio. 2019. Effects of textile dyes on health and the environment and bioremediation potential of living organisms. *Biotechnol. Res. Innov.* 3: 275–290. <https://doi.org/10.1016/j.biori.2019.09.001>
- Li, W., B. Mu, Y. Yang. 2019. Feasibility of industrial-scale treatment of dye wastewater via bio-adsorption technology. *Bioresour. Technol.*, 277:157-170. <https://doi.org/10.1016/j.biortech.2019.01.002>
- Liu, Y., Y. Kang, B. Mu, A. Wang. 2014. Attapulgite/bentonite interactions for methylene blue adsorption characteristics from aqueous solution. *Chem. Eng. J.* 237: 403–410. <https://doi.org/10.1016/j.cej.2013.10.048>
- Magdy, Y.H., H. Altaher. 2018. Kinetic analysis of the adsorption of dyes from high strength wastewater on cement kiln dust. *J. Environ. Chem. Eng.* 6: 834–841. <https://doi.org/10.1016/j.jece.2018.01.009>
- Medria, V., E. Papa, M. Mor, A. Vaccari, A. Natali Murri, L. Piatte, C. Melandri, E. Landi. 2020. Mechanical strength and cationic dye adsorption ability of metakaolin-based geopolymer spheres. *Appl. Clay Sci.* 193: 105678. <https://doi.org/10.1016/j.clay.2020.105678>
- Meziti, C., A. Boukerroui. 2012. Removal of a basic textile dye from aqueous solution by adsorption on regenerated clay. *Procedia Eng.* 33: 303–312. <https://doi.org/10.1016/j.proeng.2012.01.1208>
- Miller, G. A., S. Azad. 2000. Influence of soil type on stabilization with cement kiln dust. *Constr Build Mater.* 14(2): 89-97. [https://doi.org/10.1016/S0950-0618\(00\)00007-6](https://doi.org/10.1016/S0950-0618(00)00007-6)
- Nader, M. 2015. Surface area: Brunauer–Emmett–Teller (BET). In: *Progress in Filtration and Separation* (S. Tarleton, ed.). Academic Press, London, UK, pp. 585–608
- Netpradit, S., P. Thiraveyan, S. Twopranyoon. 2003. Application of waste metal hydroxide sludge for adsorption of azo reactive dyes. *Water Res.* 37(4): 763-772. [https://doi.org/10.1016/S0043-1354\(02\)00375-5](https://doi.org/10.1016/S0043-1354(02)00375-5)
- Oladipo, A.A., M. Gazi, S. Saber-Samandari. 2014. Adsorption of anthraquinone dye onto eco-friendly semi-IPN biocomposite hydrogel: Equilibrium isotherms, kinetic studies and optimization. *J. Taiwan Inst. Chem. Eng.* 45:653–664. <https://doi.org/10.1016/j.jtice.2013.07.013>
- Omer, O. S., M. A. Hussein, B. H. M. Hussein, A. Mgaidi. 2018. Adsorption thermodynamics of cationic dyes (methylene blue and crystal violet) to a natural clay mineral from aqueous solution between 293.15 and 323.15 K. *Arab. J. Chem.*, 11(5): 615-623. <https://doi.org/10.1016/j.arabjc.2017.10.007>
- Osman, M.A., F. M. Kishk, A. A. Moussa, H. M. Gaber. 2017. Sorption and Desorption of Atrazine on Natural Bentonite and Organically Modified Bentonite. *Alexandria Sci. Exch. J. An Int. Q. J. Sci. Agric. Environ.* 38: 271–283. <https://doi.org/10.21608/asejaiqjsae.2017.3475>
- Pai, S., M. S. Kini, R. Selvaraj. 2021. A review on adsorptive removal of dyes from wastewater by hydroxyapatite nanocomposites. *Environ. Sci. Pollut. Res.* 28:11835–11849. <https://doi.org/10.1007/s11356-019-07319-9>
- Paluszkiwicz, C., M. Holtzberg, A. Bobrowski. 2008. FTIR analysis of bentonite in moulding sands. *J. Mol. Struct.* 880: 109–114. <https://doi.org/10.1016/j.molstruc.2008.01.028>
- Pavia, D.L., G. M. Lampman, G. S. Kriz, J. R., Vyvyan. 2009. *Introduction to Spectroscopy*. 4th ed. Brooks/Cole, Belmont, CA.
- Pentrák, M., A. Czímerová, J. Madejová, P. Komadel. 2012. Changes in layer charge of clay minerals upon acid treatment as obtained from their interactions with methylene blue. *Appl. Clay Sci.* 55: 100–107. <https://doi.org/10.1016/j.clay.2011.10.012>
- Pirkarami, A., M. E. Olya. 2017. Removal of dye from industrial wastewater with an emphasis on improving economic efficiency and degradation mechanism. *J. Saudi Chem. Soc.* 21: S179–S186. <https://doi.org/10.1016/j.jscs.2013.12.008>
- Rahman, M.K., S. Rehman, O.S. B. Al-Amoudi. 2011. Literature Review on Cement Kiln Dust Usage in Soil and Waste Stabilization and Experimental Investigation. *IJSER.* 7: 77–87.
- Reddy T, R., K. S, E. T. S. L. Reddy. 2017. Spectroscopic characterization of bentonite. *J. Lasers, Opt. Photonics* 4: 171. <https://doi.org/10.4172/2469-410x.1000171>
- Şahin, Ö., M. Kaya, C. Saka. 2015. Plasma-surface modification on bentonite clay to improve the performance of adsorption of methylene blue. *Appl. Clay Sci.* 116–117: 46–53. <https://doi.org/10.1016/j.clay.2015.08.015>
- Salem, A., E. Velayi. 2012. Application of hydroxyapatite and cement kiln dust mixture in adsorption of lead ions from aqueous solution, *Ind. Eng. Chem. Res.* 18: 1216–1222. <https://doi.org/10.1016/j.jiec.2011.11.113>
- Salem, A., H. Afshin, H. Behsaz. 2012. Removal of lead by using Raschig rings manufactured with mixture of cement kiln dust, zeolite and bentonite, *J. Hazard. Mater.*, 223–224:13–23. <https://doi.org/10.1016/j.jhazmat.2012.01.002>
- Salem, W.M., W. F. Sayed, S. A. Halawy, R. B. Elamary. 2015. Physicochemical and microbiological characterization of cement kiln dust for potential reuse in wastewater treatment. *Ecotoxicol. Environ. Saf.* 119: 155–161. <https://doi.org/10.1016/j.ecoenv.2015.05.012>
- Salleh, M.A.M., D. K. Mahmoud, W. A. Karim, A. Idris. 2011. Cationic and anionic dye adsorption by agricultural solid wastes: A comprehensive review. *Desalination.* 280 (1–3):1-13. <https://doi.org/10.1016/j.desal.2011.07.019>

- Saraya, M.E.S.I., M. E. S. Aboul-Fetouh. 2012. Utilization from cement kiln dust in removal of acid dyes. *Am. J. Environ. Sci.* 8: 16–24.
<https://doi.org/10.3844/ajessp.2012.16.24>
- Sen, T.K., S. Afroze, H. M. Ang. 2011. Equilibrium, kinetics and mechanism of removal of methylene blue from aqueous solution by adsorption onto pine cone biomass of *Pinus radiata*. *Water. Air. Soil Pollut.* 218: 499–515.
<https://doi.org/10.1007/s11270-010-0663-y>
- Shehata, N., M. S. Geundi, E. A. El, Ashour, R. M. A. Abobeah. 2016. Structural Characteristics of the Egyptian Clay as a Low-Cost Adsorbent. *Int. J. Chem. Process Eng. Res.* 3: 35–45.
<https://doi.org/10.18488/journal.65/2016.3.2/65.2.35.45>
- Sikdar, D., K. S. Katti, D. R. Katti. 2008. Molecular interactions alter clay and polymer structure in polymer clay nanocomposites. *J Nanosci Nanotechnol.* 8 (4): 1638–1657.
- Sun, J., L. Qiao, S. Sun, G. Wang. 2008. Photocatalytic degradation of Orange G on nitrogen-doped TiO₂ catalysts under visible light and sunlight irradiation, *J. Hazard. Mater.* 155: 312–319.
<https://doi.org/10.1016/j.jhazmat.2007.11.062>
- Tahir, S.S., N. Rauf. 2006. Removal of a cationic dye from aqueous solutions by adsorption onto bentonite clay. *Chemosphere.* 63: 1842–1848.
<https://doi.org/10.1016/j.chemosphere.2005.10.033>
- Tekin, N., O. Demirbas, M. Alkan. 2005. Adsorption of cationic polyacrylamide onto kaolinite, Micropor. *Mesopor. Mater.* 85: 340–350.
<https://doi.org/10.1016/j.micromeso.2005.07.004>
- Toor, M., B. Jin, S. Dai, V. Vimonses. 2015. Activating natural bentonite as a cost-effective adsorbent for removal of Congo-red in wastewater. *J. Ind. Eng. Chem.* 21: 653–66. <http://dx.doi.org/10.1016/j.jiec.2014.03.033>
- Trana, H. N., S. Youb, H. Chaob. 2016. Thermodynamic parameters of cadmium adsorption onto orange peel calculated from various methods: A comparison study, *JECE.* 4:2671–2682.
<https://doi.org/10.1016/j.jece.2016.05.009>
- Vargas, A.M.M., A. L. Cazetta, A. C. Martins, J. C.G. Moraes, E. E. Garcia, G. F. Gauze, W.F. Costa, V. C. Almeida. 2012. Kinetic and equilibrium studies: Adsorption of food dyes Acid Yellow 6, Acid Yellow 23, and Acid Red 18 on activated carbon from flamboyant pods. *Chem. Eng. J.* 181–182: 243–250.
<https://doi.org/10.1016/j.cej.2011.11.073>
- Vermohlen, K., H. Lewandowski, H. D.Narres, M. J., Schwuger, 2000, Adsorption of polyelectrolytes onto oxides-the influence of ionic strength, molar mass, and Ca²⁺ ions. *Colloids Surf. A* 163: 45–53.
[https://doi.org/10.1016/S0927-7757\(99\)00429-X](https://doi.org/10.1016/S0927-7757(99)00429-X)
- Wang, S., E. Ariyanto. 2007. Competitive adsorption of malachite green and Pb ions on natural zeolite. *J. Colloid Interface Sci.* 314: 25–31.
<https://doi.org/10.1016/j.jcis.2007.05.032>
- Wong, S., N. A. Ghafar, N. Ngadi, F. A. Razmi, I. M. Inuwa, R. Mat, N. A. S. Amin. 2020. Effective removal of anionic textile dyes using adsorbent synthesized from coffee waste. *Sci. Rep.* 10: 1–13. <https://doi.org/10.1038/s41598-020-60021-6>
- Wu, F.C., R. L. Tseng, R. S. Juang. 2009. Characteristics of Elovich equation used for the analysis of adsorption kinetics in dye-chitosan systems. *Chem. Eng. J.* 150:366–373. <http://dx.doi.org/10.1016/j.cej.2009.01.014>.
- Xue, W., H. He, J. Zhu, P. Yuan, P. 2007. FTIR investigation of CTAB–Al–montmorillonite complexes. *Spectrochimica Acta Part A* 67:1030–1036.
<http://dx.doi.org/10.1016/j.saa.2006.09.024>
- Yagub, M. T., T. K. Sen, S. Afroze, H. M. Ang. 2014. Dye and its removal from aqueous solution by adsorption: a review. *Adv. Colloid Interface Sci.* 209: 172–184.
<https://doi.org/10.1016/j.cis.2014.04.002>
- Zhu, R.L., L. Z. Zhu, J. X. Zhu, F. Ge, T. Wang. 2009. Sorption of naphthalene and phosphate to the CTMAB–Al13 intercalated bentonites. *J. Hazard. Mater.* 168: 1590–1594. <https://doi.org/10.1016/j.jhazmat.2009.03.057>

المخلص العربي

إزالة صبغة الميثيلين الزرقاء من المحاليل المائية بواسطة معدن البنتونيت والتراب الإسمنتي:

دراسة مقارنة لحركية واتزان الادمصاص والديناميكا الحرارية

أحمد عبد الخالق الرفاعي

والثانية. ووجد تطابق واضح وبشكل جيد لنموذج الدرجة الثانية مع جميع التركيزات الأولية المختبرة (٥٠-٣٠٠ ملجرام/لتر). كما تم دراسة وتقييم عملية ادمصاص بواسطة النماذج المختلفة للاتزان وهي نموذج فرنديلخ، ونموذج لانجومير ونموذج تمكن. وقد توافقت النتائج التجريبية المتحصل عليها جيداً مع نموذج لانجومير. وقد أظهر البنتونيت قدرة ادمصاصية (٣٢٥٧,٣٣ مجم / جم) أعلى من المتحصل عليها بواسطة CKD (٢١٥٠,٥٤ مجم / جم). ولوحظ زيادة في كفاءة عملية ازالة صبغة الميثيلين الزرقاء لكل من المادتين المختبرين مع زيادة درجة الحرارة من ٢٩٨ إلى ٣٢٣ كلفن. وبدراسة وحساب الثوابت الثيرموديناميكية وجد أن العملية كانت تلقائية والتفاعل ماصة للحرارة. وأوضحت النتائج المتحصل عليها أن كلا المادتين فعالة ومنخفضة التكلفة من أجل إزالة صبغة الميثيلين الزرقاء، مع وجود فعالية اكبر للبنتونيت في عملية الازالة وامتياز لـCKD لعدم وجود تكلفة.

قامت الدراسة بمقارنة عملية إزالة صبغة الميثيلين الزرقاء (MB) من المحاليل المائية بواسطة معدن طبيعي هو البنتونيت (Bent) وتراب الأسمنت (CKD) كنواتج ثانوى من عملية تصنيع الاسمنت. وتم دراسة خواص معدن البنتونيت وكذلك التراب الاسمنتي بواسطة انحراف الأشعة السينية (XRD)، ومضان الأشعة السينية (XRF)، وكذلك السطح النوعي، والتحليل الطيفي بالأشعة تحت الحمراء (FTIR) وتحت الميكروسكوب الالكترونى (SEM) لتوضيح الاختلافات فى الخصائص الفيزيائية والكيميائية. أجريت تجارب الادمصاص على دفعات للمقارنة بين اداء البنتونيت وCKD لازالة صبغة الميثيلين الزرقاء تحت الظروف المختلفة من اختلاف التركيز الاولى وكميات المادة المادصة ودرجات ال pH المختلفة وتركيزات الملوحة وكذلك درجات الحرارة المختلفة. كما تم دراسة حركية الادمصاص من خلال النماذج المختلفة وهي نموذج الحركية الاسية، ونموذج Elovich ونموذج الدرجة الاولى